Turkish Journal of Earth Sciences

Volume 33 | Number 2 Article 2

1-29-2024

Microfacies, geometry and growth phases of microbial mound in Gucheng area, Southeastern Tarim Basin, China

Xu CHEN
chenxu2004@126.com

IFTIKHAR SATTI
iasatti20@gmail.com

Yuwen DONG
2810702021@qq.com

Recommended Citation

CHEN, Xu; SATTI, IFTIKHAR; and DONG, Yuwen (2024) "Microfacies, geometry and growth phases of microbial mound in Gucheng area, Southeastern Tarim Basin, China," *Turkish Journal of Earth Sciences*: Vol. 33: No. 2, Article 2. https://doi.org/10.55730/1300-0985.1902
Available at: https://journals.tubitak.gov.tr/earth/vol33/iss2/2

TÜBİTAK

Turkish Journal of Earth Sciences

http://journals.tubitak.gov.tr/earth/

Research Article

Turkish J Earth Sci
(2024) 33: 99-117

doi:10.55730/1300-0985.1902

Microfacies, geometry and growth phases of microbial mound in Gucheng area, Southeastern Tarim Basin, China

Xu CHEN[1,2,3], **Iftikhar SATTI**[4,*], **Yuwen DONG**[5]

[1]School of Geoscience, Yangtze University, Wuhan, China
[2]State Key Laboratory of Continental Dynamics, Northwest University, Xi'an, China
[3]State Key Laboratory of Geological Processes and Mineral Resources, China University of Geosciences, Wuhan, China
[4]Al Haytham Mining Company, Riyadh, Saudi Arabia
[5]Hubei Key Laboratory of Petroleum Geochemistry and Environment, Yangtze University, Wuhan, China

Received: 18.10.2022 • **Accepted/Published Online:** 24.11.2023 • **Final Version:** 29.01.2024

Abstract: A microbial mound is favorable carbonate reservoir for petroleum exploration, particularly in the deep tight reservoirs of the Tarim petroliferous basin. Due to lack of effective research methods, it is difficult to analyze its unique sedimentary structure and evolution process. In this study, , the investigation of petrographic texture, microfacies, geometry, and growth phases of microbial mound in Gucheng area, Southeastern Tarim Basin was conducted using cores, thin-sections, logging, 3D seismic data, and geochemical test data. The findings can be utilized to reconstruct dynamic evolution of the microbial mounds and discuss the controlling factors. The major results are as follows: (1) Gucheng area is located in the margin facies belt of a relatively high-energy platform, conducive to the growth and development of microbial mounds. Seven petrographic textures were identified, forming four sedimentary microfacies types: mound base, mound core, mound flat, and mound wing. (2) During the Middle and Upper Cambrian periods, four phases of microbial mound sedimentation occurred successively, with each phase superimposed in the oceanward direction. The development area covered more than 1400 km^2, with stripped distribution that extends from south to north in the plane. (3) The four phases of microbial mound complexes reflect the gradual evolution process of carbonate platform, transitioning from low angle slope to a platform margin in regional sea level regression environment. The microfacies geometry and growth phases of microbial mounds were mainly controlled by sea level change and palaeogeomorphology.

Key words: Microbial mound, geometry, growth phases, sea level regression, Southeastern Tarim Basin

1. Introduction

Microorganisms were common in geological history and played a significant role in the construction of modern reefs. Microbial communities account for approximately 80% of the total amount of organisms in the Earth's modern biosphere and similarly constitute about 80% of the Earth's life history (e.g., Burne and Moore, 1987; Riding, 2000; Tian et al., 2018; Huang et al., 2019; Tomás et al., 2019; Dylan et al., 2020; Li et al., 2021). Due to the large number, wide distribution, and diverse types of microorganisms, they have played a key role in the evolution of the Earth. From the Cambrian life explosion to the Ordovician period, the growth and development of microorganisms was the most enriched and active, arousing extensive attention and thought among geologists (e.g., Li et al., 2008; Grotzinger and Al Rawahi, 2014; You et al., 2018; Lai et al., 2020; Shen et al., 2020; Zhu et al., 2020; Hu et al., 2021). At the same time, with the global oil and gas exploration reaching deep ancient strata, an increasing number of oil and gas fields related to microbial carbonate reservoir have been discovered all over the world. Examples include the Tarim Basin, Sichuan Basin and Bohai Bay Basin in China, Santos Basin in Brazil, Oman Salt Basin and Caspian Sea Basin in Central Asia and East Siberia in Russia. Consequently, the microbial carbonate reservoir holds great significance for high-quality reservoir prediction and the success of commercial oil and gas exploration (e.g., Tull, 1997; Chesnel et al., 2016; Koeshidayatullah et al., 2016; Mannani, 2016; Schröder et al., 2016; Franchi and Frisia, 2020; Blanco et al., 2021; Zohdi et al., 2021).

Microbial mounds are local uplift of carbonate rocks formed by algae or microbial rocks, which have become an important direction for carbonate oil and gas research and a significant field for commercial oil and gas exploration in the deep strata. In 2020, the first deep exploration well in Asia (i.e. Luntan-1), exceeding 9000 m, was drilled in the

* Correspondence: iasatti@gmail.com

Tarim Basin. This deep well yields high-quality light crude oil from the Cambrian microbial mound reservoir.

The reservoir porosity value ranges from 1.6% to 6.2%, with an average value of 1.8%, and the permeability ranges from 0.02 to 4.68 mD. Despite belonging to a low porosity and low permeability reservoir, in this deep burial depth and large-scale carbonate development area, it still exhibits industrial capacity (e.g., Chesnel et al., 2016; Mannani, 2016; Deng et al., 2018; Franchi and Frisia, 2020). This confirmed that microbial mound deposits were favorable exploration targets and have significant oil and gas potential.

The Cambrian represents the relatively old sedimentary strata in the Tarim Basin. During this period, typical large marine carbonate platforms were developed in the basin. The vast eastern part of the basin was located in an open platform sedimentary environment. The microbial mound complex, widely developed in the platform margin zone, was the major carrier of high-quality oil and gas reservoirs in (super) deep strata (e.g., Deng et al., 2018; Shen et al., 2018; He et al., 2019; Ma et al., 2019). At present, relying on various high-quality data and research methods, previous studies have investigated specific aspects of the sedimentary and reservoir characteristics of microbial mounds (e.g., Shen et al., 2018; Chen et al., 2019; Ma et al., 2019). However, due to the significant depth of burial and the scarcity of deep drilling data in Cambrian, the successful drilling in Cambrian strata is limited, particularly affecting the scarcity of core data. This limitation has constrained the theoretical research on microbial mounds in Cambrian carbonate platforms, especially those in the Tarim Basin.

In addition, due to the poor quality of deep seismic data, high exploration costs, as well as its deep burial depth, ancient age, complex sedimentary structure, and diagenesis, it is difficult to fully study the microbial mound. At present, only tectonic-lithofacies palaeogeography at the basin scale had been studied in the Cambrian system (e.g., Li et al., 2015; He et al., 2017; Zhang, 2017; Cao et al., 2019; Chen et al., 2019; He et al., 2019; Hu et al., 2019). The detailed analysis of sedimentary microfacies, geometry and growth phases of microbial mound was rarely conducted, which restricted the accuracy of reservoir prediction and the deployment of exploration for microbial mounds.

In recent years, 3D seismic data and two sets of well data (i.e. wireline logs, core data, detailed test data, and production data) in Cambrian are available for the Gucheng area in the Southeastern Tarim Basin. In this study, the data are integrated to present a detailed case study of the microbial mound's sedimentary characteristic and growth evolution on relatively large spatial scales. The primary objectives of this study are as follows: 1) to analyze the petrographic texture and identify the sedimentary microfacies types of microbial mounds, 2) to reconstruct the development phases and superimposed pattern of microbial mounds, and 3) to discuss the growth process and the major controlling factors of the microbial mounds.

2. Geological setting

The Tarim Basin is a large, complex, superimposed basin formed by multistage structural- sedimentary evolution on the metamorphic basement of pre-Sinian (e.g., Lai et al., 2020). The study area is located in the east of Gucheng low uplift in the Southeastern Tarim Basin. It exhibits a continuous succession of uplift and features a large, wide, gentle nose structure inclined to the northwest (e.g., Li et al., 2008; Grotzinger and Al Rawahi, 2014; You et al., 2018; Lai et al., 2020; Zhu et al., 2020).

In the north area, there is a gentle slope transitioning to the Manjiaer depression. It is bounded by the Tazhong No.1 fault in the western part, connected with Tangguzibasi depression and Tanan uplift in the southern area, and bounded by Gucheng platform margin zone in the eastern area (Figure 1). The Tarim Basin was in a weakly extensional tectonic setting from the Cambrian to the Early Ordovician, and the typical large marine carbonate platforms were developed in the basin during this period. The sedimentary environment of the western part was in the carbonate platform facies belt, and the eastern part was in the basin facies belt, deposited dark mudstone. The southeast area of the Tarim Basin was located in the platform margin facies belt, providing a broad space for the extensive development of microbial mounds (e.g., Li et al., 2008; Grotzinger and Al Rawahi, 2014; Lai et al., 2020; Shen et al., 2020; Zhu et al., 2020). The tectonic rudiment of the Gucheng uplift was formed by the tectonic activities at the end of Ordovician. The tectonic framework of the Gucheng area, which was generally higher in the southeast and lower in the northwest, was formed during the late Paleozoic tectonic event movement (Figure 2).

The drilling data reveals that the sedimentary strata thickness in the Gucheng area is significant, exceeding 10 km in some areas. This formation is well-developed from the Cambrian to the Quaternary period. From bottom to top, the sediments consist of marine carbonate rocks from the Cambrian to the Ordovician, marine clastic rocks from the Silurian to the Carboniferous, lacustrine clastic rocks in the Permian, and continental fluvial clastic rocks from the Mesozoic to the Cenozoic (e.g., Tull, 1997; Blanco et al., 2021; Hu et al., 2021). The Cambrian system is the key strata of deep oil and gas exploration; the drilling depth can reach 7000 m, and the lithology is primarily carbonate rock (e.g., Franchi and Frisia, 2020; Chesnel et al., 2021). The Cambrian system is subdivided into six formations. The lower Yuertusi Formation is composed of thick black mudstone and marl with stable distribution throughout the basin and high-quality deep source rock. Multiple sets of reservoir and cap assemblages are developed in the middle and upper Cambrian, and the reservoir lithology is mainly algal (mound) microbial dolomite (e.g., Deng et al., 2018; Ma et al., 2019) (Figure 2).

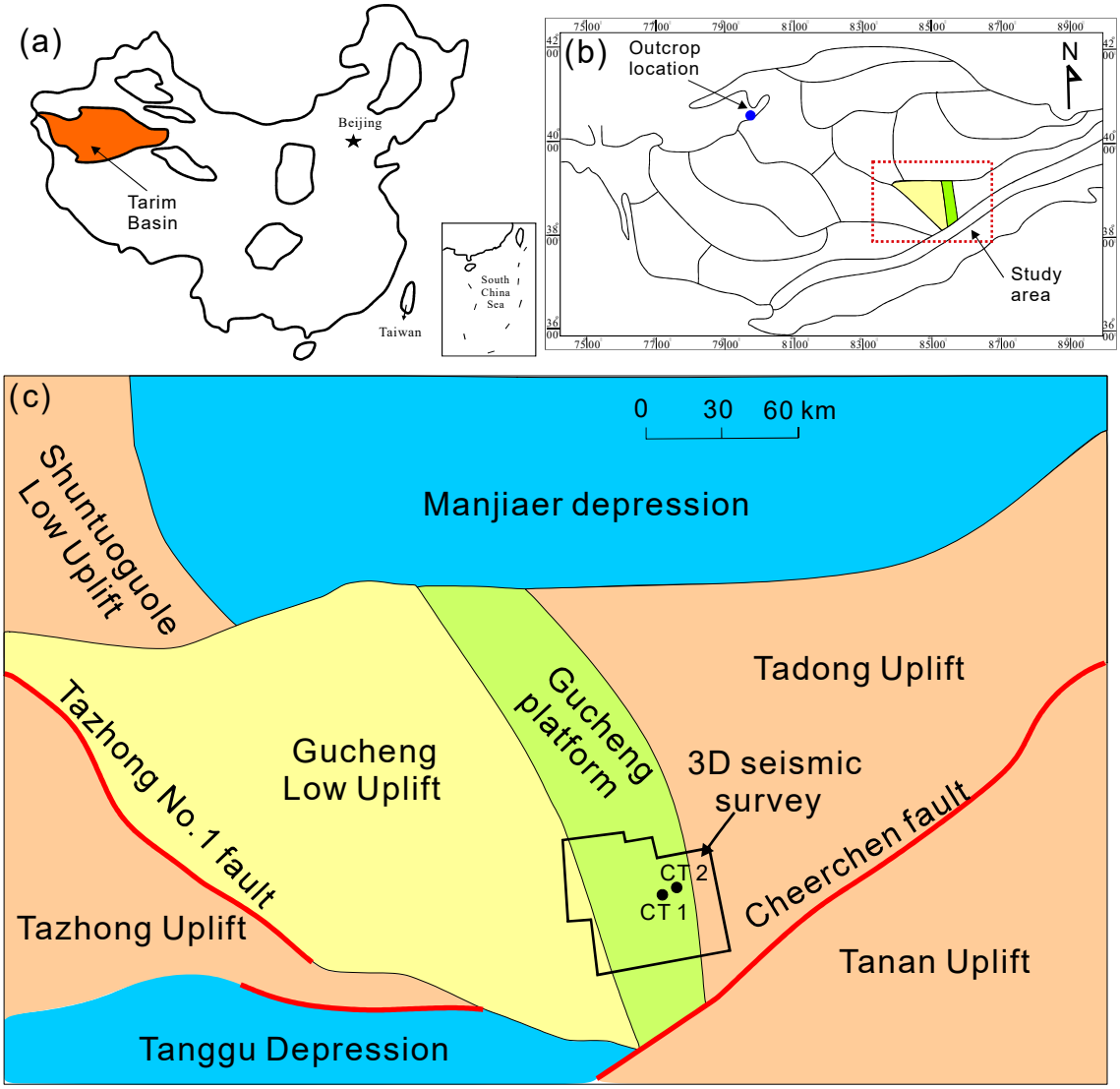

Figure 1. Regional location of the Tarim Basin in the western China (a), tectonic setting of the Tarim Basin (b), and the Gucheng low uplift, well location and the 3D seismic survey location (c).

3. Dataset and methods

This study was based on core data, thin-section observations, geochemical testing, well logging, and high-resolution 3D seismic data. There were only two wells (CT1, CT2) drilled into the Cambrian with approximately 21.56 m long cores. Wireline log data used in this study include gamma ray (GR) without uranium (KTH), photoelectric absorption cross section index (PE), deep and shallow lateral resistivity formation resistivity (LLD, LLS), sonic travel time (AC), density (Den), ratio of thorium to uranium content (Th/U), and the mineral content of $CaCO_3$ and $MgCO_3$. These data were used for petrography texture, lithologic composition, reservoir analysis, sedimentary microfacies, and depositional cycles (i.e. upward-fining and upward-coarsening cycles). Furthermore, $\delta^{13}C$ carbon isotope and porosity interpretation curve was used for sedimentary and reservoir analysis.

Sixty-six samples from two wells were systematically selected to cover all microbial mound petrography and cut into thin sections for microscopic petrographic studies. Alizarin Red-S was applied to one-third of the thin sections to distinguish between calcite and dolomite. Additionally, partial microbial mound reservoir samples were impregnated with blue resin and cut into thin sections to observe the pores under the microscope. The major carbonate grains, including their petrographic and diagnostic criteria, were in accordance with the terminology defined by Flügel (2010). The identification lithofacies was

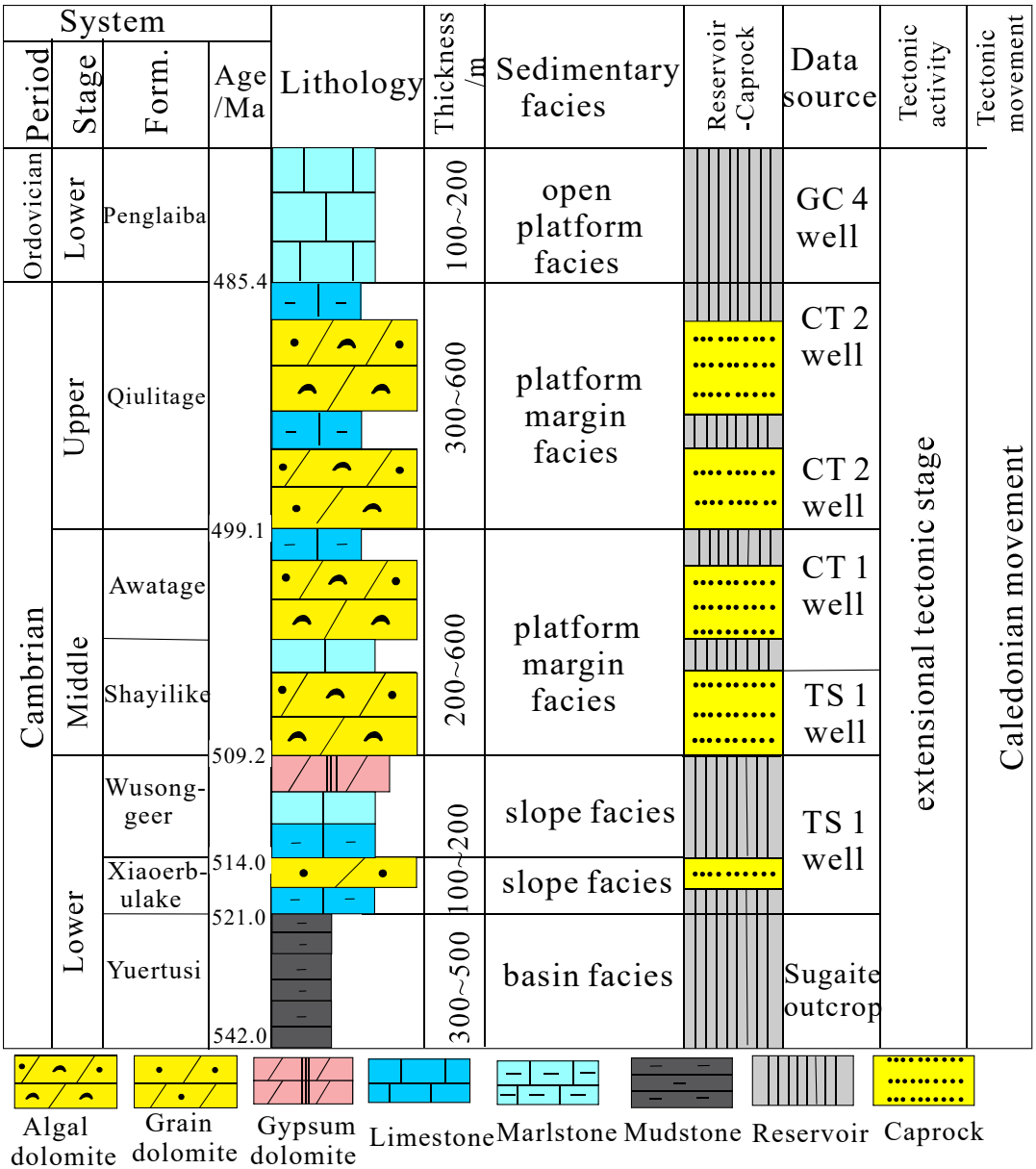

Figure 2. Cambrian general stratigraphy, lithology, and tectonic evolution in Gucheng area, Southeastern Tarim Basin.

based on the modified Dunham classification by Wright (1992). Petrography and lithofacies associations were constructed and correlated across the carbonate platform to determine the sedimentary environment and facies.

Through the carbon stable isotope test, the composition and variation of carbon isotope in this area are analyzed, and the palaeoclimate, palaeoceanic, and palaegeographic environment are explained. The isotope samples consist mainly of fresh rock samples, and they should avoid calcite veins, recrystallization sites, and weathering development. This ensures that the stable isotope composition characteristics of the original sedimentary environment can be accurately reflected. A total of 8 rock samples were collected and tested. The sample processing and testing were completed by the Isotope Geochemistry Laboratory of Yangtze University. The carbon and oxygen isotopic compositions of the samples were analyzed using GasBench II and Mass spectrometer MAT253. The bottle containing the appropriate number of samples was placed in the GasBench II thermostat. Six drops of phosphoric

acid were added after purging the air. After at least 4 h of constant temperature reaction, the CO2 generated by the reaction was separated by helium column at 70 ºC and then entered the mass spectrometer MAT253 to determine the carbon isotope value. The accuracy of carbon isotope values was 0.01‰.

The study area, covering approximately 4000 km^2, was entirely covered by 3D seismic data . This data is characterized by an effective frequency band between 5 and 55 Hz, a peak frequency of 25 Hz, a vertical seismic resolution of 30–45 m, and a two-way travel time between 3 and 4.5 s within the interval containing the total Cambrian formation in the Gucheng area. Based on the results of synthetic seismograms, nine regional strata were detailed interpreted as follows: Tϵ(the bottom of the Yuertusi Formation in the Lower Cambrian), Ty^0 (the bottom of Shayilike Formation in the Middle Cambrian), Ty^1 (the bottom of Awatage Formation in the Middle Cambrian), Ty^2 (the bottom of Upper Qiulitage Formation in the Upper Cambrian), Ty^3 (the bottom of Lower Qiulitage Formation in the Upper Cambrian), Ty^4 (the top of Lower Qiulitage Formation in the Upper Cambrian), TO^1 (the bottom of Lower Ordovician), TO^2 (the bottom of Upper Ordovician), TO^3 (the top of Upper Ordovician). The outer morphology and inner structure of microbial mounds were identified and characterized through the analysis seismic amplitude envelope interfaces (SAEI). The macroscopic characteristics were predicted using seismic facies analysis.

At present, only a few wells have been drilled into the Cambrian system, but there are a large number of regional two-dimensional survey lines and three-dimensional seismic data in the study area. Through horizon tracking, correlation, and interpretation, it is easier to obtain the transverse distribution characteristics of the microbial mound, providing valuable information for the restoration of palaeogeomorphology. The residual strata thickness method was used to restore the palaeogeomorphology of the Cambrian. First, the marker layer adjacent to the microbial mounds was selected as the base level for layer flattening. Secondly, the effect of carbonate sedimentary environment is considered. Finally, the analysis focused on the relationship between stratum contacts, internal reflection structures, and variations in real stratum thickness. The study also involved the division of palaeogeomorphic and topographic units, as well as three-dimensional visualization characterization. Above all, the growth phases, evolution process, and major controlling factors of microbial mounds were analyzed at different stages in the Cambrian.

4. Results

4.1. Petrographic texture

4.1.1 Dendritic texture

It is mainly characterized by the dendritic microbial texture of epiphytes, and the dendritic lithology is mainly formed by the skeleton of epiphytes themselves (e.g., Wright, 1992; Song et al., 2014). The shrubby, in situ tufted or clumpy micromorphology is observed in the outcrops, where sparry cementation and primary pores are developed in the dendritic lattice (Figure 3a). The drilling data reveals that the dendritic texture is often branched phylloid monomer or cluster spherical fragment, which is often associated with high-energy debris, such as oolitic particle (Figures 3b–3d). It reflects the high energy hydrodynamic environment under strong wave action (e.g., Song et al., 2014; Huang et al., 2016; Chen et al., 2017).

4.1.2. Spongy texture

In the outcrop section, it is characterized by light gray to gray-white thick layer or massive dolomite with spongy and honeycomb texture. The microbe cavity is well-developed (Figure 3e). This type of dolomite is primarily composed of foamed cyanobacteria (e.g., Huang et al., 2016), and the foam bodies are generally round and irregularly oval. They are associated with gravel and sand debris, indicating a relatively strong hydrodynamic environment.

4.1.3. Particle texture

The particle texture is related to wave breaking and washing action, and it is formed in the relatively strong hydrodynamic environment (e.g., Chen et al., 2017). Particle composition mainly includes gravel debris, sand debris, bioclasts, and oolitic texture. The gravel debris contains microbiological debris, such as epiphyte debris (Figures 3c and 3d). The bioclasts are mainly cyanobacteria microbe particles with coelomere-like foam layer texture. The particle size of sand and oolitic particles is generally approximately 1 mm, the sort and roundness of the particle are good (Figures 3f–3i). The interior of the clasts is dark, and there are signs of cyanobacteria and algae microbial adhesion activity (Figures 3j–3k).

4.1.4. Coagulation texture

It is a typical type of microbial texture, which is closely related to the deposition and formation of microbial mounds. This texture is related to the capture and adhesion of clasts and other particle by cyanobacteria (e.g., Luo et al., 2013; Huang et al., 2016). Due to the characteristics of particle agglutination, the interior of the particle appears dark, and the sort and roundness of the particle are poor. The shape is irregular, and the boundary is uneven and not clear, with obvious characteristics of cyanobacteria microbe adhesion. The coagulation is generally larger than 1 mm, and its shape differs from sparry cementation in the coagulations (Figures 3l and 3m). The coagulation texture is mainly developed in the shallow subtidal zone with turbulent environment.

4.1.5. Laminated texture

The laminated texture is one of the most common microbial textures in the study area, characterized by alternating light and dark patterns (e.g., Zhang et al.,

2021). It is composed of three different lithological layers, including spherulitic alga adhesion layer, algal adhesion, and sparry cementation spherulitic layer, and sparry adhesion silty layer (Figure 3n). The first layer is composed of silty dolomite with a high micrite content, formed through microbe capture and adhesion. The second layer also exhibits a typical feature of microbial capture with densely distributed spherules in layers, and the boundary of the spherules is not clearly defined. The spherules are mainly algal adhesion and locally sparry cementation. The third layer consists of fine dolomite formed through the cementation of poorly sorted silty dolomite. The laminated texture reflects the turbulent water environment, ranging from weak to strong, and generally exhibits characteristics of weak water energy.

4.1.6. Spherulitic texture

It is a spherical or ellipsoidal particle with a dark micrite composition and small particle size, generally less than 0.2 mm. It exhibits well-sorted fuzzy particle boundary and scattered distribution; it is mostly associated with fine clastic composition (Figure 3o). This type of microbial structure is related to microbial coagulation, reflecting weak hydrodynamic environment. (e.g., Bai et al., 2017, 2018; Lan et al., 2019)

4.1.7. Silicified texture

Siliceous (mineralized) texture is a typical petrographic texture in microbial mounds. It is produced in the form of siliceous clumps (Figure 3p) and some of the siliceous rocks contain dolomite pseudo crystals.

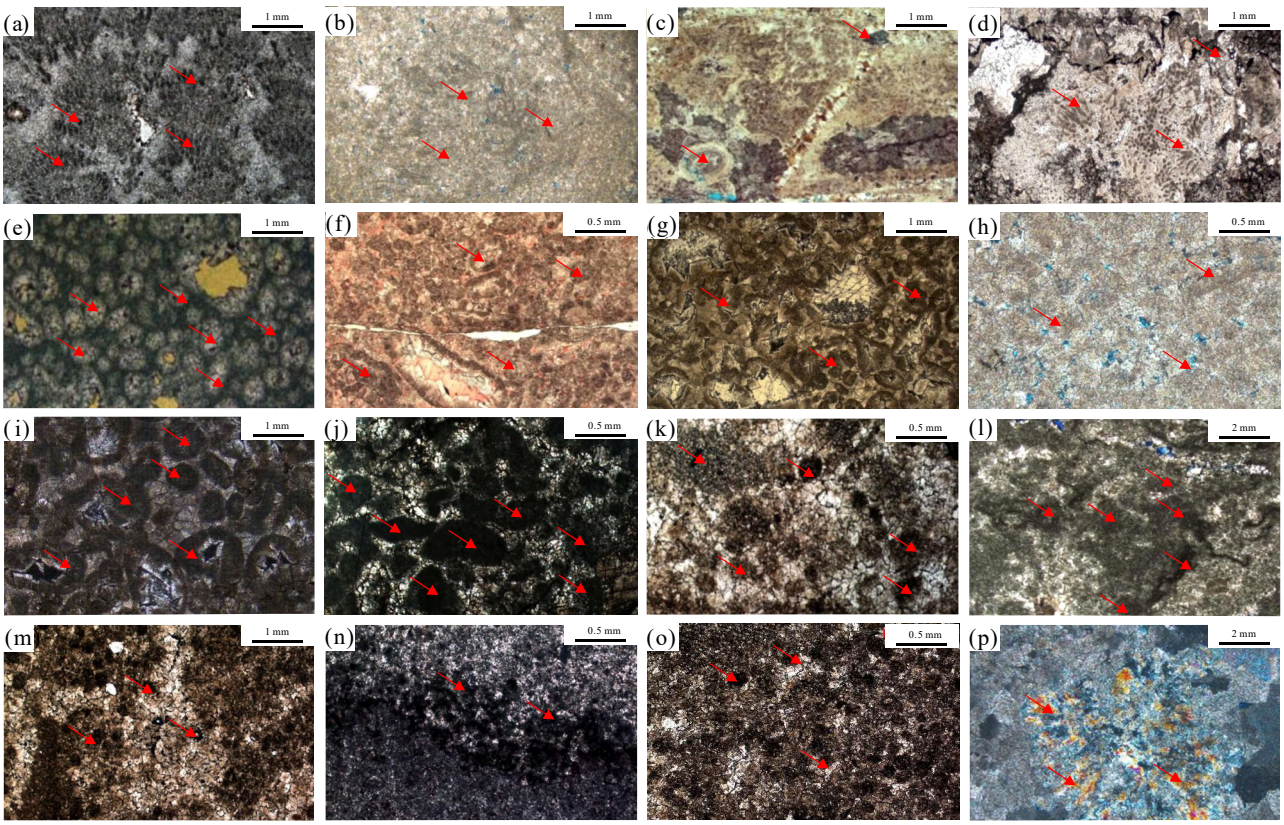

Figure 3. Petrographic texture of microbial mound in Gucheng area, Southeastern Tarim Basin. (a) Clumpy and dendritic epiphyte dolomite mound core, Sugaite outcrop; (b) clumpy and dendritic algae sand debris dolomite mound core, CT2, 6272.77 m; (c) dendritic sand debris and oolitic dolomite mound core, CT1, 6875 m; (d) dendritic gravel debris dolomite mound core, CT2, 662.63 m; (e) spongy dolomite mound core, Sugaite outcrop; (f) bioclastic particle dolomite mound flat, CT2, 6730 m; (g) sand debris particle dolomite mound flat, CT2, 6729.9 m; (h) particle dolomite mound flat, CT1, 6372.7 m; (i) bioclastic particle dolomite mound flat, CT2, 6729 m; (j) spherulitic and sand debris dolomite mound flat, CT1, 7006 m; (k) gravel and sand debris coagulation dolomite mound wing, CT1, 7125.6 m; (l) cyanobacteria coagulation dolomite, mound wing, Sugaite outcrop; (m) gravel and sand debris coagulation dolomite mound wing, CT1, 7125.6 m; (n) laminated dolomite mound wing, CT1, 7142.7 m; (o) spherulitic and sand debris dolomite mound base, CT1, 7257 m; (p) spherulitic alga adhesion and sand debris dolomite locally silicified clumps, mound flat, CT3, 7369.28 m.

4.2. Microfacies types

4.2.1. Microbial mound base

It was developed in the lower subtidal belt, where the relative sea level began to decline during deposition. However, the water depth remained relatively deep, and the water energy was not strong. It was located at the bottom of microbial mound, characterized by medium thick layer and massive deposits. The lithology consists of silty dolomite with microbial sand debris and spherulitic texture. The type of cementation between grains is parry cementation with dispersed spherulitic material. The reservoir exhibits high organic matter content and underdeveloped pores, indicating a relatively deep water and weak energy hydrodynamic environment during the initial deposition of microbial mounds (Figures 3o–4).

4.2.2. Microbial mound core

It was developed on top of the mound base, the relative sea level continued to fall during deposition. Under moderate or strong turbulent hydrodynamic conditions, microorganisms began to grow quickly, forming obviously thick mound deposits. The lithology is microbiological dolomite, and the petrography texture is varied, including dendritic texture, coagulation texture, and particle texture. The particle size is generally coarser (Figures 3a–3f). The KTH (GR (gamma ray) value of uranium removal) is low, ranging from 1.21 to 11.75 API (American Petroleum Institute), with an average of about 2.94 API. The curve shape changes from a high-sharp peak to a low, flat profile. The values of $\delta_{13}C$ gradually changes from a positive bias to a negative bias from bottom to top, ranging from –1.05‰

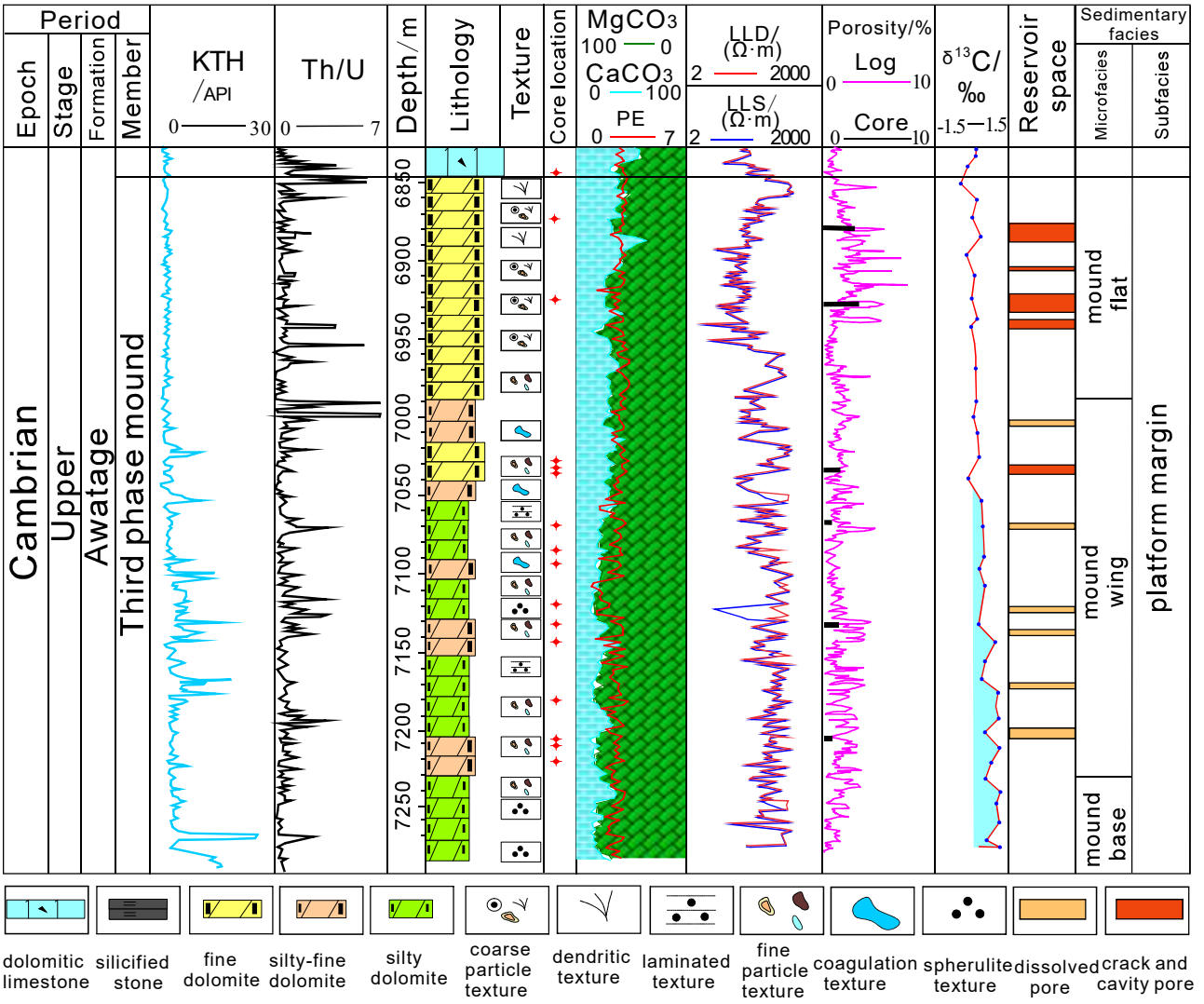

Figure 4. CT1 well comprehensive interpretation of petrographic texture, microfacies types and reservoir physical property.

to 0.29‰, with an average of –0.226‰. This indicates the sedimentary environment with lower sea level, shallower water, and stronger energy. In addition, the Th/U ratio of GR spectral logging at the top of the microbial mound core increases sharply (greater than 7), revealing the existence of a weathered layer at the top of the microbial mound, indicating the exposure to oxidation and denudation in the regressive environment (Figures 4 and 5). The mound core reservoir consists of fine dolomite with algal or sand debris, and the dissolution pores or fractures are developed in the breccia (Figures 6a–6e).

4.2.3. Microbial mound flat

It was developed on the top of microbial mound, appearing as a thick dome deposit. At this stage, due to the further decline of the relative sea level and the continuous enhancement of water energy, the top of the microbial mound was near the storm wave base and generally stopped growing. The unconsolidated microbial dolomite formed in the early time underwent fragmentation due to wave action, subsequently reaccumulating on the upper or lateral surfaces of the microbial mound, forming a large number of particle texture dolomite, referred to as mound flat deposition. The lithology is composed of fine dolomite with oolitic and particle texture. It is mainly composed of unconsolidated microbial rock washed, broken, and redeposited by strong wave action near the wave base, so the granularity is coarse with sparry cementation (Figures 3g–3j).

The KTH value is low, ranging from 1.01 to 9.88 API, with an average of 2.54 API, and the curve shape is low and flat. From bottom to top, the values of $\delta_{13}C$ gradually change from positive bias to negative bias, ranging from –1.15‰ to 0.23‰, with an average of –0.226‰. This includes the microbial mound flat located in the shallow water, high-energy deposition area, as compared to the deep water carbonate sedimentary environment (Figures 4 and 5).

The reservoir is composed of fine dolomite with particle texture. Intergranular pores, intragranular pores, and dissolution pores are well-developed in large quantities, and some of them are filled with silica (Figures 6f–6i).

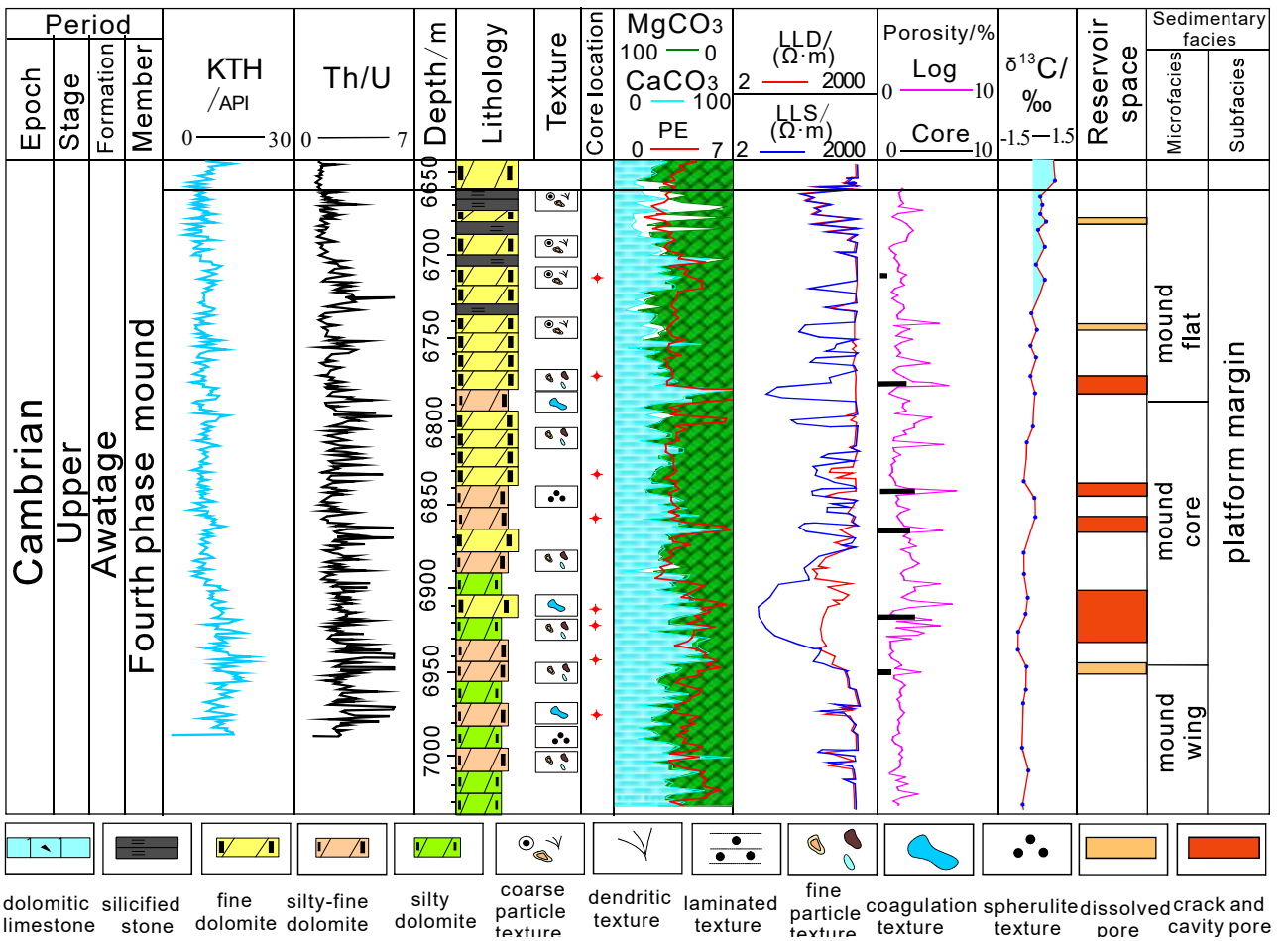

Figure 5. CT2 well comprehensive interpretation of petrographic texture, microfacies types and reservoir physical property.

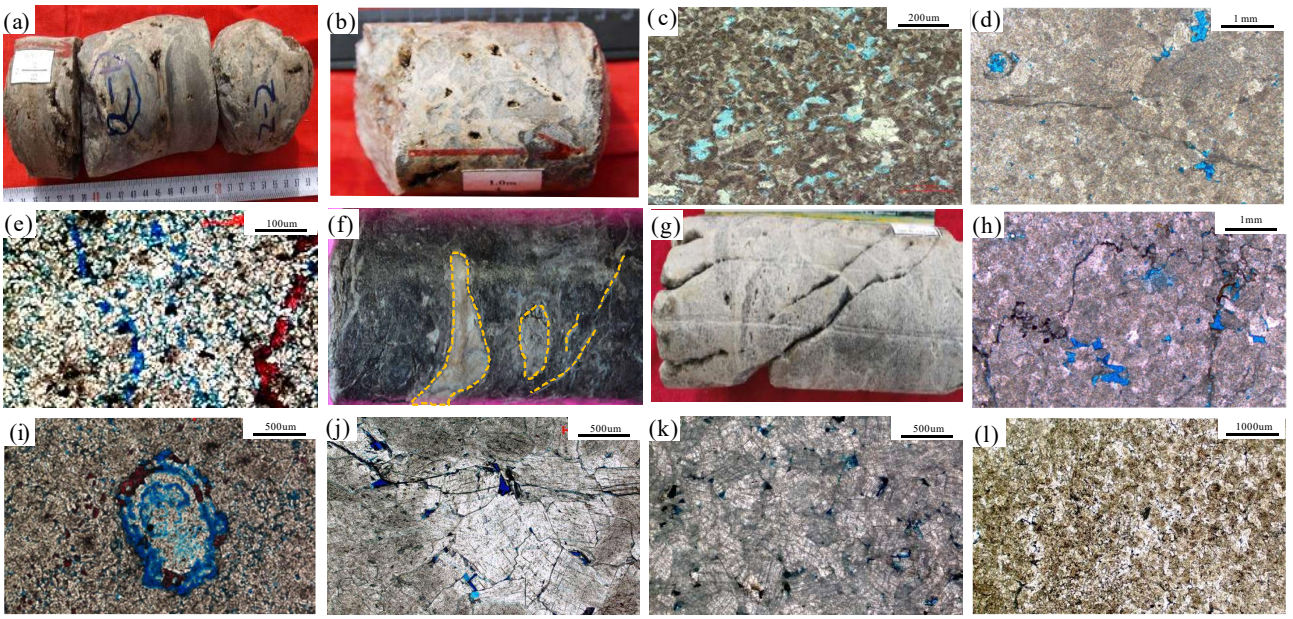

Figure 6. Lithologic composition, reservoir pore type of microbial mound in Gucheng area, Southeastern Tarim Basin. (a) Breccia dolomite, dissolution pore and cave, mound core, CT1, 6875.43 m, core; (b) breccia dolomite, dissolution pore and cave, mound core, CT1, 6876.28 m, core; (c) algal adhesion dolomite, intergranular (dissolved) pores, mound core, CT2,6 823.25 m, thin section; (d) algal sand debris dolomite, intragranular dissolved pore, CT2,7372.2 m, thin section; (e) silty dolomite, dissolution fissure and intergranular dissolution pore, mound core, CT1, 7140.35 m, thin section; (f) karst cave and fracture, filled with siliceous, mound flat, CT2, 6733.10 m, core; (g) algal lattice dissolution pore and high angle fracture mound flat, CT1 well, 6720.10 m, core; (h) suture and fracture filling, intergranular dissolved pore, mound flat, CT2, 7070.8 m, thin section; (i) biofilm casted pore and intergranular (dissolved) pore, mound flat, CT1, 7041 m, thin section; (j) residual sand debris silty to fine dolomite, intergranular (dissolved) pore, mound wing, CT1 well, 6847 m, thin section; (k) silty to fine dolomite, locally developed intergranular pore, mound wing, CT1, 7 142.74 m, thin section; (l) spherulitic silty to fine dolomite, intergranular (dissolved) pore, mound wing, CT1, 6847 m, thin section.

4.2.4 Microbial mound wing

It was developed at the edge or flank of the microbial mound core. The lithology is composed of silty and fine dolomite, including sand debris particle texture, coagulation texture, and a small amount of microspherulitic. There are growth traces of cyanobacteria in the particles, the sort and roundness of debris in the particle are poor, with sparry cementation and fine particle size (Figures 3k–3n).

The KTH is relatively high, ranging from 1.67 to 21.81 API with an average of 6.16 API. From bottom to top, the curve shape changes from microtoothed and low flat to peak high value. $\Delta_{13}C$ value shows a positive deviation ranging from 0.036‰ to 1.41‰, with an average value of 0.724‰. This reflects the sedimentary environment of sea level rise and weak water energy (Figure 4).

The reservoir lithology consists of silty to fine dolomite, and the reservoir space comprises intercrystalline pores, a few structural dissolution fractures, and intercrystalline dissolution pores (Figures 6j–6l).

4.3. Reservoir physical property

4.3.1 Microbial mound core

According to the core physical interpretation, it is found that the reservoir porosity ranges from 1.3 to 7.2, with an average of 3.4. Additionally, the permeability ranges from 0.02 to 3.62 mD. According to the Oil and Gas industry standard of the People's Republic of China, the physical property classification standard of carbonate reservoir in SY/T6285-2011 (e.g., Deng et al., 2018), it belongs to low porosity and low permeability reservoir (Figures 4 and 7; Table 1).

4.3.2 Microbial mound flat

The reservoir porosity ranges from 1.5 to 8.1, with an average of 4.6, and the permeability ranges from 0.02 to 5.88 mD, which are also low porosity and low permeability reservoirs (Figures 4 and 7; Table 1).

4.3.3 Microbial mound wing

The value of reservoir porosity is low, ranging from 0.8 to 2.1, with an average of about 1.3. The logging permeability value ranges from 0.01 to 1 mD, indicating that it is an ultralow porosity and ultralow permeability reservoir (Figures 4 and 7; Table 1).

4.4. Seismic reflection characteristics

Through the analysis of synthetic calibration and seismic reflection characteristics of microbial mounds, the geometry, including external morphology and internal structure, is identified and characterized. Compared with

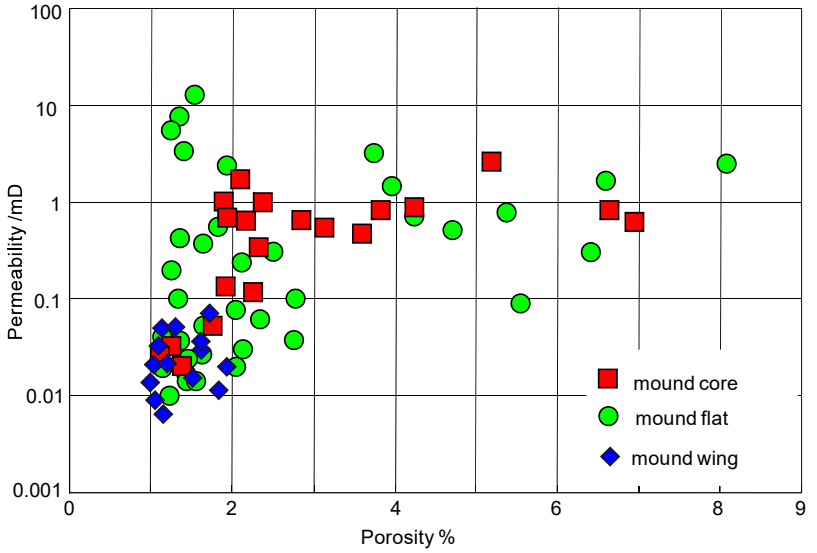

Figure 7. Crossplot between porosity and permeability of microbial mound microfacies types in Gucheng area, Southeastern Tarim Basin.

Table 1. The typical characteristics of different microfacies types in Gucheng area, Southeastern Tarim Basin.

Microfacies types	Petrographic texture	KTH /API	$\delta_{13}C_{PDB}$ (‰)	Porosity	Permeability /mD
Microbial mound base	Silicified texture, laminated texture, coagulation texture	No data			
Microbial mound core	Dendritic texture, coagulation texture, spongy texture	1.21–11.75 ave: 2.94	- 1.05–0.29 ave: –0.226	1.3–7.2 ave: 3.4	0.02–3.62
Microbial mound flat	Particles texture, Dendritic texture	1.01–9.88 ave: 2.54	–1.15–0.23 ave: –0.226	1.5–8.1; ave: 4.6	0.02–5.88
Microbial mound wing	Coagulation texture, Spherulite texture	1.67–21.81 ave: 6.16	0.036–1.41 ave: 0.724	0.8–2.1 ave: 1.3	0.01–1

the surrounding rock, the vertical stratum thickness of microbial mounds significantly increases . Multiphased microbial mound deposits are superimposed horizontally on different scales, exhibiting seismic facies characteristics such as mound shape, wedge shape or lens shape (e.g., Shi et al., 2019; Zhang et al., 2019; Zheng et al., 2020). The velocity of the microbial mound exceeds that of the surrounding rock, leading to a significant seismic wave impedance difference at the top interface. This difference corresponds to a strong peak reflection. Simultaneously, seismic wave polarity reversal or event pinchout phenomenon occurs in the direction of the vast ocean, reflecting the boundary of microbial mound growth toward the ocean side. These features exhibit the typical characteristics of seismic amplitude envelope interfaces (SAEI). Consequently, the external morphology and distribution scope of microbial mounds are clarified through SAEI analysis (Figure 8).

The SAEI of microbial mound is characterized by medium-strong amplitude and continuous reflection. The reflection characteristics on the top, bottom and inside of the SAEI are obvious and easy to identify and track. The onlap and covered seismic reflections are well-developed

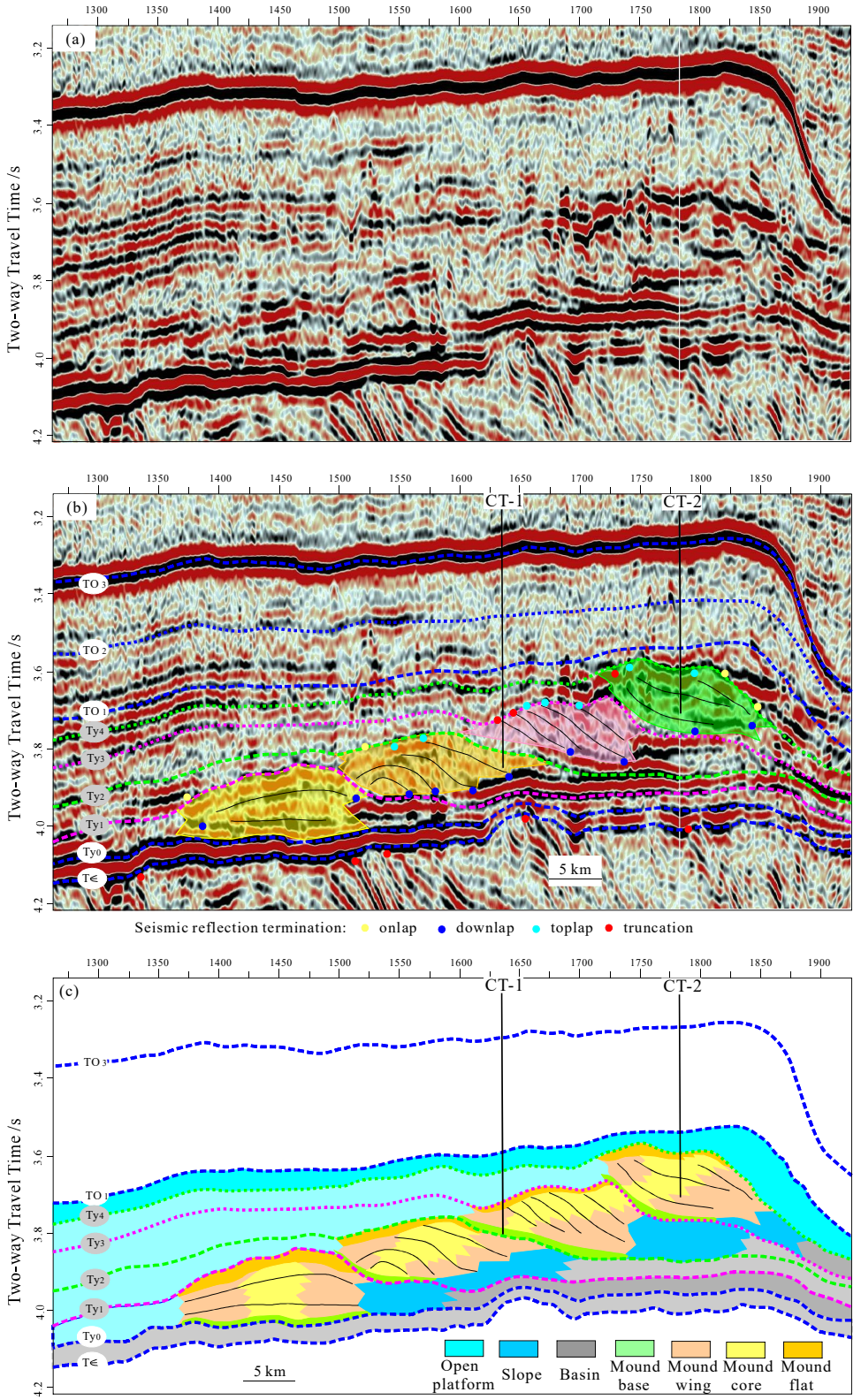

Figure 8. Seismic reflection characteristics of platform margin belt past CT1-CT2 well. (a) Original profile, (b) interpreted profile, and (c) the microbial mound seismic facies interpretation section (see the section location in Figure 9).

on the top of SAEI and the downlap and truncation seismic reflection termination are well-developed at the bottom of SAEI. The inner side of SAEI exhibits low frequency, weak amplitude signals, indicating progradation or local disorderly reflection, converging to the mound wing. Based on the special seismic reflection above, the SAEI of microbial mounds is tracked and interpreted in detail. It is not difficult to find that a total of four SAEIs, named Ty1, Ty2, Ty3 and Ty4, correspond to the development of four phases of microbial mound complexes in the Middle and Upper Cambrian (Figure 8). Through the 3D view of microbial mounds in different phases, it can be clearly seen that the microbial mounds are gradually progradational toward the direction of the ocean basin. The overlapped area covered more than 1400 km^2 with stripped distribution from south to north in the geographical plane (Figure 9).

5. Discussion

5.1. Development phases and superimposition patterns of microbial mounds

Microbial mounds are mostly formed by algae or fungal microorganisms, and their internal seismic reflection amplitude energy is weak; most of them are intermittent, blank, or disorderly structures (e.g., Zheng et al., 2020). However, in the process of microbial in situ growth, due to changes in palaeogeomorphology and relative sea level, the frequent interlayers between mound and flat areas are visible, and a variety of vertically overlapping styles may appear, such as accretion, progradation or retrogradation (e.g., Ngia et al., 2019). Based on the above characteristics, the developmental phases and superposition patterns of the Middle and Upper Cambrian microbial mounds in the study area were analyzed (Figure 8b; Table 2).

5.1.1 The first phase

The top interface of the first phase mound is characterized by low frequency, strong amplitude, and high continuous reflection. The regional distribution of the top interface is stable. The SAEI of the first phase mound is complete in shape, with a clear outer morphology that is easy to compare and trace. The outer morphology exhibits a symmetrical and dome-shaped structure, converging towards the mound wings on both sides. The interior of the microbial mound is characterized by weak amplitude, low frequency, and medium continuous reflection. It tends to exhibit layered features, showing a vertically accreted 'sandwich' geometry (Figure 8b). This pattern revealed that the palaeogeomorphology was wide and gentle, and the rate of sea level rise was roughly consistent with the growth rate of microbial mounds. The shape of the first phase microbial mound was clearly defined, with a growth height of about 400 m and a width of approximately 9.5 km. It exhibited stripped distribution from south to north in the plane, extending about 3.1 km in front of the first mound. Due to the low tectonic position and the potential risk of cap rock, no drilling has been conducted yet (e.g., Lan et al., 2019).

5.1.2 The second phase

The second phase mound began to grow on the mound wing and slope adjacent to the first phase and it was obviously influenced by the palaeogeomorphology after the deposition of the first phase microbial mound. The second phase is subdivided into two phases. In the early phase, under the background of steep slope after the deposition of the first phase mound, the sedimentary hydrodynamic was strong and the microbial mound in

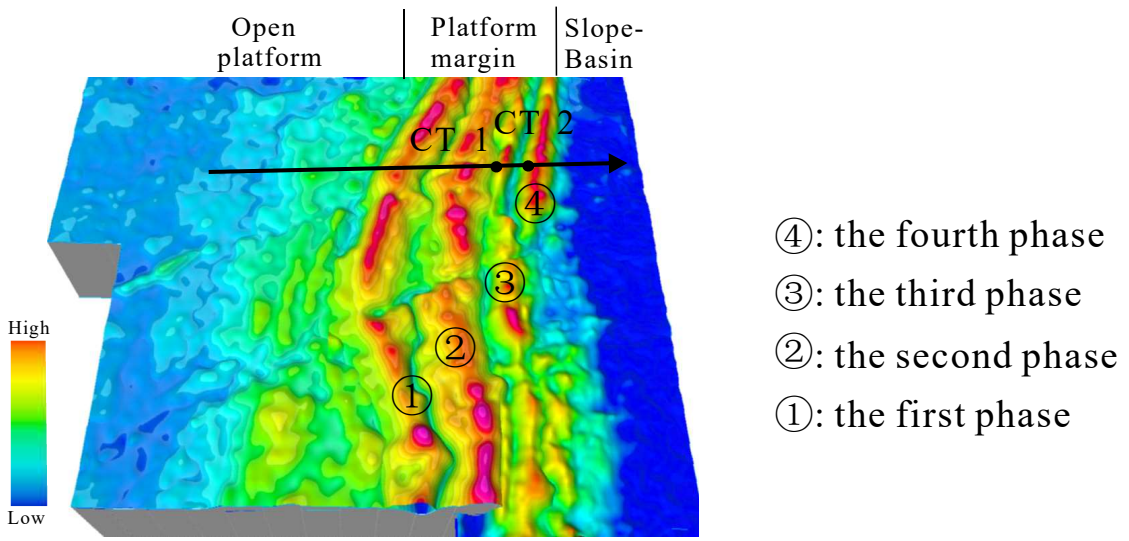

Figure 9. 3D view of four phases of microbial mounds in Gucheng area, Southeastern Tarim Basin.

Table 2. Development phases and macroscopic distribution characteristics of microbial mound in Gucheng area, Southeastern Tarim Basin.

Phase	Period	Thickness range (m)	Average thickness (m)	Width range (km)	Average width (km)	Buried depth (m)
Fourth	Upper Qiulitage Formation in the Late Cambrian	80~560	320	2.3~8.1	4.4	6300~7625
Third	Lower Qiulitage Formation in the Late Cambrian	130~580	360	5.8~9.2	7.1	6500~7750
Second	Awatage Formation in the Middle Cambrian	120~600	380	7~15.3	10.4	6650~7625
First	Shayilike Formation in the Middle Cambrian	220~660	400	6.8~12.1	9.5	7025~8300

lateral direction was narrow. The geometry primarily involved vertical accretion, and the seismic reflection character exhibited discontinuity and disorder. In the later phase, with the rapid growth and reproduction of microorganisms, the microbial mound was characterized by asymmetrical mound. The seismic reflection changed to weakly continuous and gentle progradation reflection, and vertical accretion to weak progradation geometry was formed (Figure 8b).

Under the background of steep slope, the growth rate of microorganisms was slightly greater than or equal to the rate of sea level rise. The deposition thickness is larger, the growth height was more than 380 m, and the total width was about 10.4 km.

5.1.3 The third phase

Significantly different from the previous two phases, the third phase mound exhibited wedge progradation on the slope of the previous mounds. The seismic reflection was characterized by medium-weak amplitude, medium continuity, and layered character, in which the top of microbial mound was truncated, and the stable and complete mound core was not developed (Figure 8b). CT1 drilling data also revealed the presence of weathered layer on top of the microbial mound, reflecting exposure and denudation due to sea level decline (Figure 5). At this time, the distribution scale of microbial mound became smaller, the growth height was about 360 m, and the width was 7.1 km.

5.1.4 The fourth phase

On the basis of the third phase mound, the top interface exhibited low frequency and strong amplitude reflection, making it easy to track and characterize. The mound was incomplete, and the scale was smaller (Figure 8b). The growth height was about 320 m, and the length was about 4.4 km.

5.2. Sedimentary evolution

5.2.1 Regional Sea level regression background

The Southeastern Tarim Basin was located in the open platform sedimentary environment during the Cambrian (e.g., Song et al., 2014; Ngia et al., 2019; Tang et al., 2019). With stable basement subsidence and less fault development under the regional sea-level regressive background, the microbial mound deposits developed on gentle slope of the platform margin. In the western part of the study area, deposits of open platform, semiconfined platform, and platform margin facies were developed as well as high energy facies zones such as grain beach inside platform and microbial mounds at the platform margin (e.g., Wright, 1992; Song et al., 2014; Huang et al., 2016). In the eastern part, deposits of calcareous debris flow slope and basin facies were developed (e.g., Qiao et al., 2019; Zhu et al., 2020) (Figure 10).

5.2.2 Palaeogeomorphic research

The variation characteristics of palaeogeomorphology were often a comprehensive reflection of hydrodynamic conditions, sedimentary rate and accommodate space. The growth and evolution of microbial mounds were very sensitive to the palaeogeomorphology (e.g. Macnaughton et al., 2018; Jin et al., 2020; Guido et al., 2021). Therefore, the growth and evolution characteristics of microbial mounds were analyzed by restoring the palaeogeomorphic morphology of different phases in the Cambrian. Currently, only two wells have been drilled in the Cambrian system in the study area. However, there are a large number of regional 2D survey lines and 3D seismic data, which can provide a lot of geological information for the restoration of palaeogeomorphology.

The method of residual stratum thickness was used to restore the palaeogeomorphology of Cambrian. Firstly, the marker layer adjacent to the microbial mound was

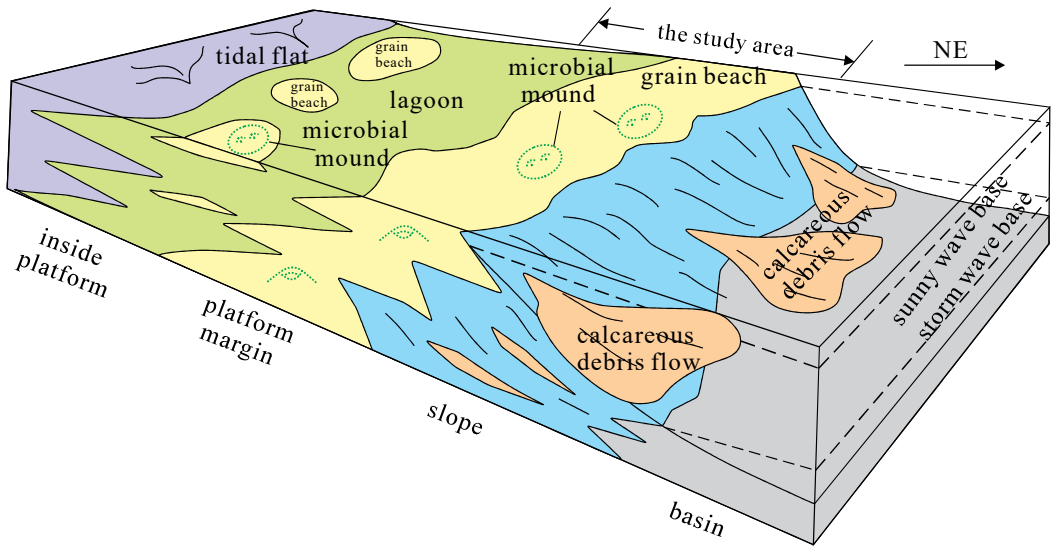

Figure 10. Regional depositional model of microbial mound in the carbonate platform in Gucheng area, Southeastern Tarim Basin.

selected as the datum level, and the layer was flattened. The mudstone of Yuertusi Formation in the Lower Cambrian was stably distributed in the whole basin, and it was also the largest regional transgressive marker in the basin. The seismic reflection was characterized by low frequency, high amplitude, and continuous reflection, which can be traced in the whole region. In the study area, the Yuertusi formation in the Lower Cambrian can be defined as the datum level (Figure 11). Secondly, the carbonate sedimentary environment was considered in the study. During the Cambrian period, the study area was characterized by stable marine carbonate deposit, exhibiting strong compaction and weak tectonic activity. The study area was located in an open platform environment characterized by minimal uplift and denudation, and so the role of uplift and denudation can be ignored. Finally, based on the fine structural interpretation result of seismic data, the division of palaeogeomorphic topographic units and 3D visualization were carried out, focusing on the analysis of strata contact relationship within reflection character and real stratum thickness recovery. Among them, the real stratum thickness from the top of the Lower Cambrian to the selected datum level (the Yultusi formation) was the palaeogeomorphology before the deposition of the first phase mound. Similarly, the real stratum thickness from the top of the first phase mound to the Yultusi Formation was the palaeogeomorphology before the deposition of the second microbial mound. By analogy, the palaeogeomorphology before each phase mound deposition were obtained respectively (Figure 12).

5.2.3 Sedimentary evolution

From the Cambrian to early Ordovician, the carbonate platform in the study area had undergone the characteristics of low-angle slope platform margin and submerged platform. Four phases mound complex deposition were developed in the carbonate platform margin, which successively prograded and overlapped in the direction of the vast ocean. The growth and sedimentary evolution characteristics were shown as follows (Figure 12).

In the early Cambrian, the Tarim basin was in the epicontinental marine sedimentary environment. During this period, the basin experienced a large-scale transgression, resulting in the formation of thick mudstone deposits in the Yurtusi Formation in the whole basin (e.g., Ngia et al., 2019; Zheng et al., 2020). Tectonically, the study area was located on the slope of carbonate platform, with a low angle inclined to the vast ocean on the whole, with no obvious slope break. The study area was in a low energy and reductive sedimentary environment (e.g., Song et al., 2014; Chen et al., 2017).

In the Shayilike Formation of the Middle Cambrian, after transgression, the relative sea level slowly began to decline, and the palaeotopography was presented as a slight topographic relief in the study area, which provided basic conditions for the formation of platform margin. During this period, the gentle slope platform was gradually evolved into platform margin, which was conducive to the growth and development of microbial mounds. At this stage, the sedimentary environment energy was still weak and the accommodate space was sufficient. The rate of sea

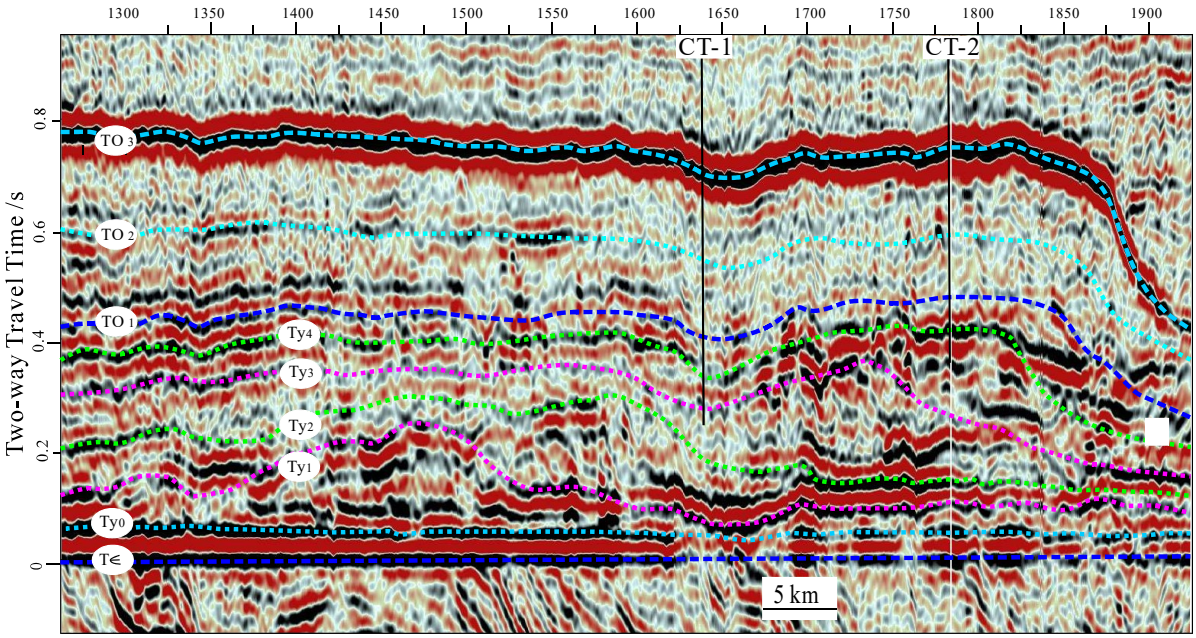

Figure 11. Seismic interpretation section past CT1-CT2 well shows flatten base of Cambrian (see the section location in Figure 9).

level rise was roughly consistent with the growth rate of algae or fungi microorganisms, the growth pattern was mainly vertical catch-up and accretion type. When the microbial mounds were close to or exposed to sea level, the development of microbial mounds was stopped, and the first phase mound was formed. In the Awatage Formation of the Middle Cambrian, the second phase mound was developed in the wing front of the first phase mound. As the palaeogeomorphology in the microbial mound colluvial rocks became steeper, the accommodate space become larger, and the hydrodynamic conditions became stronger, which was conducive to the rapid development of microorganisms. The growth of the second phase mound was accretion and weak progradation character.

In the lower part of Qiulitage Formation of the Upper Cambrian, with the further development of carbonate platform, the third microbial mound was wedged, prograded, and deposited on the platform margin slope. During this period, the sedimentary palaeogeomorphology was steep, the sedimentary hydrodynamic condition was strong and the microorganism grew rapidly, showing the progradation characteristics in the direction of the vast ocean. The development of microbial mounds was terminated when it was exposed to sea level. In the upper part of Qiulitage Formation of the Upper Cambrian, the fourth phase mound was developed with typical progradation characteristics, and the growth scale was decreased. At the end of Cambrian, the transgression intensified again and the growth of microbial mounds was stopped. The type of platform was gradually changed to the gentle slope platform, and the study area was located in the open platform limestone deposits environment.

5.3. Controlling factors

Based on the above analysis, it was not difficult to find that growth and development of microbial mounds in the Middle and Upper Cambrian were affected by factors such as sea level change, water depth, sequence stratigraphy, palaeogeomorphology, sedimentation, and others. The vertical distribution of microbial mounds was influenced by sea level change, water depth and sequence stratigraphy, whereas the lateral distribution was influenced by palaeogeomorphic change and sedimentary facies. Overall, the growth and development of microbial mounds was mainly controlled by sea level change and palaeogeomorphology.

The palaeogeomorphology of Gucheng area was characterized by high in the west and low in the east (e.g., Zhang et al., 2021). The sedimentary facies of microbialites were predominantly developed in the higher part of the geomorphology, representing the relatively uplifted area of the platform margin facies belt, with little or no development in the low-lying area. The microbial mounds were developed horizontally and superposed with each other. The thickness and scale of the microbial mounds in the platform margin facies belt were large. Additionally, changes in palaeogeomorphology also contributed to the lithological differences in microbialites during different phases.

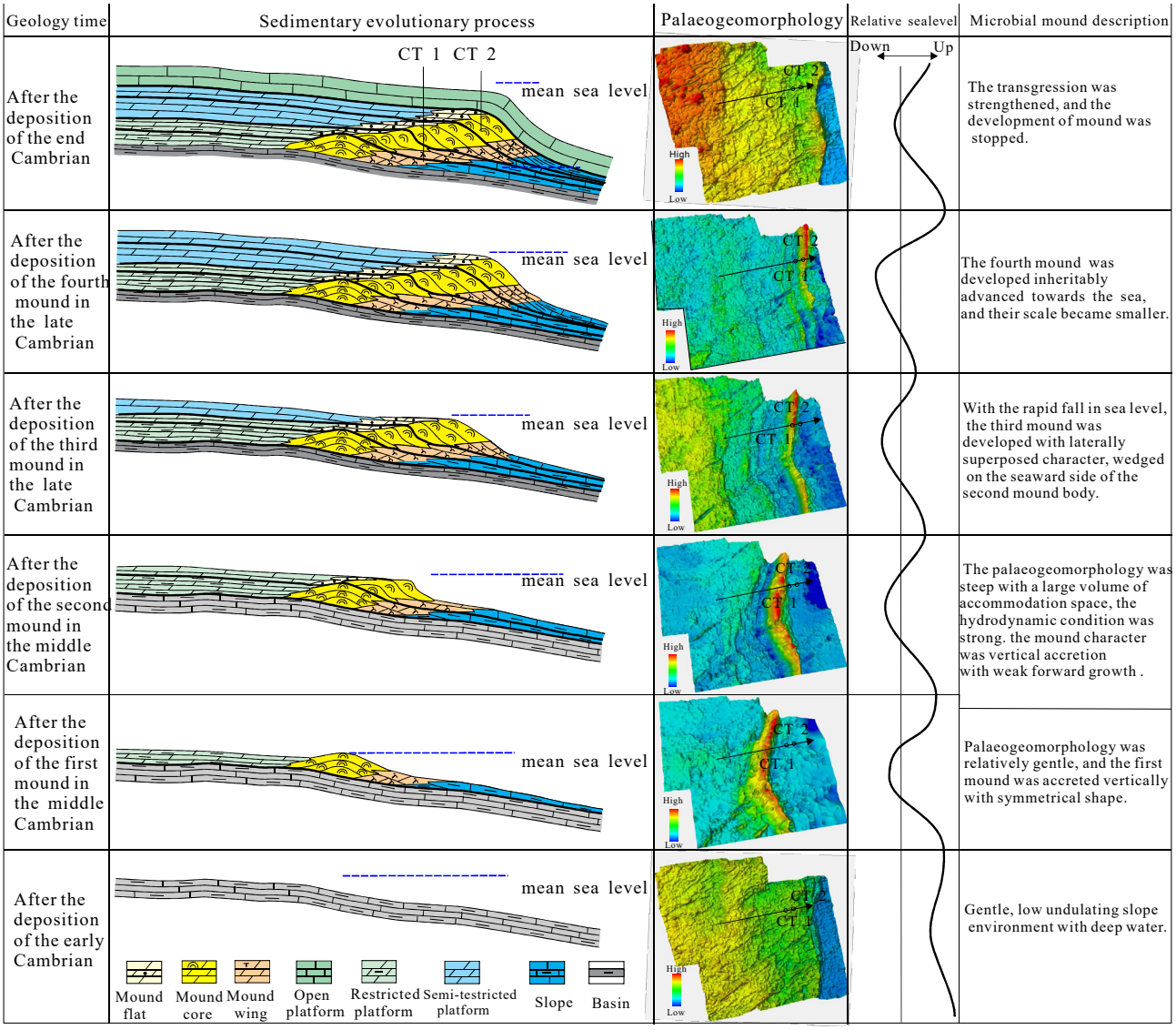

Figure 12. Microbial mound growth and evolution at the Cambrian platform margin in Gucheng area, Southeastern Tarim Basin.

Microbial carbonate rocks were usually formed in the environment of medium to high energy and were mainly formed in the upper part of subtidal zone and intertidal zone (e.g., Wright, 1992). The changes of sea level and the resulting changes of water depth, salinity, hydrodynamic conditions, and the sequence division played an important role in the formation and development of microbialites in Gucheng area. The change in sea level controlled the vertical sequence of microbialites. The microfacies and strata changes in vertical microbialites are very sensitive to the sea level change. During a sea level rise, the water depth became deeper, the water environment was not suitable for microbial growth, and the microbialites did not develop. When the sea level began to fall, the microbialites began to develop and gradually developed the mound base, mound core and mound flat. The vertical sequence of multistage microbial mounds was developed with the fluctuation of several sea levels. With the continuous accumulation of sediment, when the sediment was near the wave base surface, the seawater environment was no longer suitable for microbial development and the growth of microbialites stopped.

6. Conclusion

The microfacies, geometry, and growth phases of microbial mounds developed on the carbonate platform in the Gucheng area, Southeastern Tarim Basin, were identified on the basis of the integrated investigation involving petrographic texture, microfacies types, seismic reflection and geomorphology of the Cambrian microbial mounds.

(1) On the platform, seven typical petrographic textures of microbial mound based on macro- and microfabrics were identified. In the Gucheng area, four types of sedimentary microfacies were divided, representing mound base, mound core, mound flat, and mound wing deposits, respectively.

(2) In the Middle and Late Cambrian, the Gucheng area was located in a relatively high-energy platform margin facies belt, which was conducive to the growth and development of microbial mounds. Four phases of microbial mound complexes became evident, successively superimposed in the direction of the vast ocean area of more than 1400 km^2, occurring in north-south planar stripes.

(3) The evolution of platform margin zone was mainly controlled by the sea level change and sedimentary palaeogeomorphology. The first phase mound body was formed on a gentle slope platform with the characteristics of vertical accretion and symmetrical mound shape. The second phase mound body was developed on steeply premound colluvial rock, the geometry involved vertical accretion with weak progradational growth, forming an asymmetrical mound. The third phase mound was wedge-shaped in front of the previous mounds. The last phase mound showed smaller-scale development. When the transgression was intensified again at the end of Cambrian, the growth of microbial mounds stopped.

Funding

This research was funded by Opening Foundation of State Key Laboratory of Continental Dynamics at Northwest University (grant number 22LCD20), Open Foundation of State Key Laboratory of Geological Processes and Mineral Resources (grant number GPMR-2022-07), and College Students Innovation and Entrepreneurship Program (no. Yz2022019).

Data availability

Data is available upon request from the corresponding author.

Conflicts of interest

The authors have no conflicts of interest to declare.

Acknowledgments

The authors express gratitude to the anonymous reviewers whose valuable feedback contributed to enhancing the quality of our paper.

References

Bai Y, Luo P, Liu W, Zhai X, Zhou C (2018). Characteristics and main controlling factors of microbial carbonate reservoir: a case study of upper member of lower Cambrian Xiaerbulak formation in Aksu area, Tarim basin. China Petroleum Exploration 23 (4): 95-106. https://doi.org/10.3969/j.issn.1672-7703.2018.04.011

Bai Y, Luo P, Wang S, Zhou C, Zhai X et al. (2017). Structure characteristics and major controlling factors of platform margin microbial reef reservoirs: a case study of Xiaoerbulak Formation, Lower Cambrian, Aksu area, Tarim Basin, NW China. Petroleum Exploration and Development 44 (3): 349-358. https://doi.org/10.1016/S1876 -3804(17)30044-7

Blanco FS, Cózar P, Sanz López J (2021). Development of a Mississippian–Lower Pennsylvanian isolated carbonate platform within the basinal griotte facies of the Cantabrian Mountains, NW Spain. Facies 67 (3): 1-26. https://doi.org/10.1007/s10347-021- 00629-w

Burne RV, Moore LS (1987). Microbialites: Organosedimentary deposites of benthic communities. Palaios 2: 241-254. https://doi.org/10.2307/3514674

Cao YH, Wang S, Zhang YJ, Yang W, Yan L et al. (2019). Petroleum geological conditions and exploration potential of Lower Paleozoic carbonate rocks in Gucheng area, Tarim Basin, China. Petroleum Exploration and Development 46 (6): 1099-1114. https://doi.org/10.11698/PED.2019.06.08

Chen Y, Shen AJ, Pan L, Zhang J, Wang XF (2017). Features, origin and distribution of microbial dolomite reservoirs: a case study of 4 th Member of Sinian Dengying Formation in Sichuan Basin, SW China. Petroleum Exploration and Development 44 (5): 745-757. https://doi.org/10.11698/PED.2017.05.05

Chen YQ, YanW, Han CW, Yan L, Ran QG et al. (2019). Structural and sedimentary basin transformation at the Cambrian/Neoproterozoic interval in Tarim Basin: Implication to subsalt dolostone exploration. Natural Gas Geoscience 30 (1): 43-54. https://doi.org/10.11764/j.issn.1672-1926.2018.10.016

Chesnel V, Samankassou E, Merino OT, Fernández LP, Villa E et al. (2016). Facies, geometry and growth phases of the Valdorria carbonate platform (Pennsylvanian, northern Spain). Sedimentology 63 (1): 60-104. https://doi.org/10.1111/sed.12221

Deng SB, Guan P, Li BH, Liu PX, Chen YQ (2018). Sedimentary Texture and Formation Process of the Lower Cambrian Platform Marginal Zone in the Tarim Basin, NW China. Acta Sedimentologica Sinica 36 (4): 706-721. https://doi.org/10.1111/sed.12221

Dylan W, Sami N, Kimberly DM, Silvina S, Stefan VL et al. (2020). Depositional evolution of an extinct sinter mound from source to outflow, El Tatio, Chile. Sedimentology, 406, 1-27. https://doi.org/10.1016/j.sedgeo.2020.105726

Flügel E (2010). Microfacies of carbonate rocks: analysis, interpretation and application. Springer-Verlag, Berlin Heidelberg. https://doi.org/10.1007/978-3-662-08726-8

Franchi F, Frisia S (2020). Crystallization pathways in the Great Artesian Basin (Australia) spring mound carbonates: Implications for life signatures on Earth and beyond. Sedimentology 67: 2561–2595. https://doi.org/10.1111/sed.12711

Grotzinger J, Al Rawahi Z (2014). Depositional facies and platform architecture of microbialite-dominated carbonate reservoirs, Ediacaran–Cambrian Ara group, Sultanate of Oman. AAPG Bulletin 98 (8): 1453-1494. https://doi.org/10.1306/02271412063

Guido A, Palladino G, Sposato M, Russo M, Prosser G et al. (2021). Reconstruction of tectonically disrupted carbonates through quantitative microfacies analyses: an example from the Middle Triassic of Southern Italy. Facies 67 (3): 1-25. https://doi.org/10.1007/s10347-021-00631-2

He F, Lin CS, Liu JG, Zhang ZL, Zhang JL et al. (2017). Migration of the Cambrian and Middle-Lower Ordovician carbonate platform margin and its relation to relative sea level changes in southeastern Tarim Basin. Oil & Gas Geology 38 (4): 711-721. https://doi.org/10.1007/s10347-021-00631-2

He ZL, Yun L, You HD, Peng S, Zhang H et al. (2019). Genesis and distribution prediction of the ultra-deep carbonate reservoirs in the transitional zone between the Awati and Manjiaer depressions, Tarim Basin. Earth Science Frontiers 26 (1): 13-21. https://doi.org/10.13745/j.esf.sf.2018.12.20

Hu AP, Shen AJ, Zheng JF, Wang X, Wang XF (2021). Classification, sedimentary environment and sedimentary model of microbialites. Marine Origin Petroleum Geology 26 (1): 1-15. https://doi.org/10.3969/j.issn.1672-9854.2021.01.001

Hu MY, Sun CY, Gao D (2019). Characteristics of tectonic-lithofacies paleogeography in the Lower Cambrian Xiaoerbulake Formation, Tarim Basin. Oil & Gas Geology 40 (1): 12-23 https://doi.org/10.11743 /ogg20190102

Huang QY, Hu SY, Pan WQ, Liu W, Zhang YQ et al. (2016). Characteristics and controlling factors of the Cambrian carbonate reservoirs in Bachu area, Tarim Basin, NW China. Natural Gas Geoscience 27 (6): 982-993. https://doi.org/10.11764/j.issn.1672-1926.2016.06.0982

Huang QY, Hu SY, Pan WQ, Wei L, Chi S et al. (2016). Sedimentary characteristics of microbial mounds and their control on reservoir development: a case study of the Lower Cambrian Xiaerbulak formation in Keping-Bachu area, Tarim Basin. Geological exploration 36 (6): 21-29. https://doi.org/10.3787/j.issn.1000-0976.2016.06.003

Huang WT, Zhang YL, Guan CQ, Miao ZW, Gong EP et al. (2019). Role of calcimicrobes and microbial carbonates in the Late Carboniferous (Moscovian) mounds in southern Guizhou, South China. Journal of Palaeogeography 8 (4): 28-41. https://doi.org/10.1186/s42501-019-0041-7

Jin MD, Li BS, Zhu X, Dai L, Jiang Z et al. (2020). Characteristics and main controlling factors of reservoirs in the fourth member of Sinian Dengying Formation in Yuanba and its peripheral area, northeastern Sichuan Basin, SW China. Petroleum Exploration and Development 47 (6): 28-38. https://doi.org/10.1016/S1876-3804(20)60127-1

Koeshidayatullah A, AlRamadan K, Hughes GW (2016). Facies mosaic and diagenetic patterns of the early Devonian (Late Pragian–Early Emsian) microbialite-dominated carbonate sequences, Qasr Member, Jauf Formation, Saudi Arabia. Geological Journal 51: 704-721. https://doi.org/10.1002/gj.2678

Lai J, Wang S, Zhang CS, Wang G, Yuan C et al. (2020). Spectrum of pore types and networks in the deep Cambrian to Lower Ordovician dolostones in Tarim Basin, China. Marine and Petroleum Geology 112: 104081. https://doi.org/10.1016/j.marpetgeo.2019 .104081

Lan C, Xu ZH, Ma XL, Hu C, Zou H et al. (2019). Development and distribution of mound-shoal complex in the Sinian Dengying Formation, Sichuan Basin and its control on reservoirs. Acta Petrolei Sinica 40 (9): 1069-1084. https://doi.org/10.7623/syxb201909005

Li A, Ju LB, Zhang LY (2008). Relationship between hydrocarbon accumulation and Paleo-Mesozoic tectonic evolution characteristics of Gucheng Lower uplift in Tarim Basin. Journal of Jilin University (Earth Science Edition) 48 (2): 545-555. https://doi.org/10.13278/j.cnki.jjuese.20170259

Li JZ, Tao XW, Bai B, Huang S, Song W et al. (2021). Geological conditions, reservoir evolution and favorable exploration directions of marine ultra-deep oil and gas in China. Petroleum Exploration and Development 48 (1): 52-67. https://doi.org/10.1016/S1876-3804(21)60005-8

Li PW, Luo P, Song JM, Jin T, Wang G (2015). Characteristics and main controlling factors of microbial carbonate reservoirs: a case study of Upper Sinian-Lower Cambrian in the northwestern margin of Tarim Basin. Acta Petrolei Sinica 36 (9): 1074- 1089. https://doi.org/10.7623/syxb201509005

Luo P, Wang S, Li PW, Song JM, Jin TF et al. (2013). Research status and prospect of microbial carbonate reservoir. Acta Sedimentologica Sinica 31 (5): 807-823. https://doi.org/10.14027/j.cnki.cjxb.2013.05.005

Ma NB, Jin SL, Yang RZ, Meng L, Wang L et al. (2019). Seismic response characteristics and identification of fault karstreservoir in Shunbei area, Tarim Basin. Oil Geophysical Prospecting 54 (2): 398-403. https://doi.org/10.13810/j.cnki.issn.1000-7210.2019.02.019

Macnaughton RB, Hagadorn JW, Dott RH (2018). Cambrian wave-dominated tidal-flat deposits, central Wisconsin, USA. Sedimentology 66 (5): 1-18. https://doi.org/10.1111/sed.12546

Mannani I (2016). The role of micrites in the Sinemurian (lower Jurassic) sponge-microbialite mounds from Foum Tillicht, central High Atlas, Morocco. Bollettino della Societa Paleontologica Italiana 55 (3): 157-169. https://doi.org/10.4435/BSPI.2016.14

Ngia NR, Hu MY, Gao D (2019). Tectonic and geothermal controls on dolomitization and dolomitizing fluidflows in the Cambrian-Lower Ordovician carbonate successions in the western and central Tarim Basin, NW China. Journal of Asian Earth Sciences172: 359-382. https://doi.org/10.1016/j.jseaes.2018.09.020

Qiao Z, Shen A, Ni X, Zhu Y, Sun X et al. (2019). Types of mound-shoal complex of the Lower Cambrian Xiaoerbulake Formation in Tarim Basin, northwest China, and its implications for exploration. Oil and Gas Geology 40 (2): 392-402. https://doi.org/10.11743/ogg20190217

Riding R (2000). Microbial carbonates: the geological record of calcified bacterial- algal mats and biofilms. Sedimentology 47 (supp.1): 179-214. https://doi.org/10.1046/j.1365-3091.2000.00003.x

Schröder S, Ibekwe A, Saunders M, Dixon R, Fisher A (2016). Algal–microbial carbonates of the Namibe Basin (Albian, Angola): implications for microbial carbonate mound development in the South Atlantic. Petroleum Geoscience 22 (1): 2014-2083. https://doi.org/10.1144/petgeo2014-083

Shen AJ, Fu XD, You Z, Zheng XP, Wei L et al. (2018). A study of source rocks & carbonate reservoirs and its implication on exploration plays from Sinian to Lower Paleozoic in the east of Tarim Basin, northwest China. Natural Gas Geoscience 29 (1): 1-16. https://doi.org/10.11764/j.issn.1672-1926.2017.08.019

Shen AJ, Zhang Y, Feng ZH, Zheng XP, Zhu M et al. (2020). Geological understandings and exploration prospects of carbonate reservoirs in Gucheng area, Tadong, Tarim Basin. China Petroleum Exploration 25 (3): 96-106. https://doi.org/0.3969/j.issn.1672-7703.2020.03.009

Shi PZ, Wang ZY, Dong Y, Fan KY (2019). The classification, characteristics and development model and coupling relation with different accommodation space of platform margin reef: a case study of L_2 member of Lianglitage Formation in the eastern Tazhong area, Tarim Basin. Natural Gas Geoscience 30 (5): 673-685. https://doi.org/10.11764/i.issn.1672-1926.2018.12.016

Song JM, Luo P, Yang SS, Yang D, Zhou CM et al. (2014). Reservoirs of lower Cambrian microbial carbonates, Tarim basin, NW China. Petroleum Exploration and Development 41 (4): 404-414. https://doi.org/10.1016/S1876-3804(14)60051-3

Tang H, Kershaw S, Tan XC, Liu H, Li F et al. (2019). Sedimentology of reefal buildups of the Xiannvdong Formation (Cambrian Series 2), SW China. Journal of palaeogeography 8 (2): 170-180. https://doi.org/CNKI:SUN:GUDL.0.2019-02-005

Tian L, Cui HF, Liu J, Zhang N, Shi X et al. (2018). Early-Middle Cambrian paleogeography and depositional evolution of Tarim Basin. Oil & Gas Geology 39 (5): 1011-1021. https://doi.org/10.11743 /ogg20180515

Tomás S, Aurell M, Bádenas B, Bjorge M, Duaso M et al. (2019). Architecture and Paleoenvironment of Mid-Jurassic Microbial–Siliceous Sponge Mounds, Northeastern Spain. Journal of Sedimentary Research 89 (2): 110-134. https://doi.org/10.2110/jsr.2019.5

Tull SJ (1997). The diversity of hydrocarbon habitat in Russia. Petroleum Geoscience 3(4): 315-325. https://doi.org/10.1144/petgeo.3.4.315

Wright VP (1992). A revised classification of limestones. Sediment. Geology 76: 177–185. https://doi.org/10.1016/0037-0738(92)90082-3

You XL, Sun S, Lin CS, Zhu JQ (2018). Microbial dolomite in the sabkha environment of the Middle Cambrian in the Tarim Basin, NW China. Australian Journal of Earth Sciences 65 (1): 109-120. https://doi.org/10.1080/08120099.2018.1408031

Zhang JL (2017). Carbonate sequence sedimentary evolution and control of sea level: a case study of Ordovician in the Gucheng area, Tarim Basin. Natural Gas Industry 37 (1): 46-53. https://doi.org/10.3787/j.issn.1000-0976.2017.01.005

Zhang J, Hu M, Feng Z, Li Q, He XX et al. (2019). Types of the Cambrian platform margin mound-shoal complexes and their relationship with paleogeomorphology in Gucheng area, Tarim Basin, NW China. Petroleum Exploration and Development 48 (1): 94-105. https://doi.org/10.1016/S1876-3804(21)60008-3

Zhang Y, Li Q, Zheng XP, Li YL, Shen AJ et al. (2021). Types, evolution and favorable reservoir facies belts inthe Cambrian-Ordovician platform in Gucheng-Xiaotang area, eastern Tarim Basin. Acta Petrolei Sinica 42 (4): 447-465. https://doi.org/10.7623/syxb202104003

Zheng J, Pan W, Shen A, Yuan W, Zhu Y et al. (2020). Reservoir geological modeling and significance of Cambrian Xiaoerblak formation in Keping outcrop area, Tarim Basin, NW China. Petroleum Exploration and Development 47 (3): 499-511. https://doi.org/10.1016/S1876-3804(20)60071-4

Zhu KD, Zhang Y, Lin T, Wang YC, Zheng XP et al. (2020). Pore-throat heterogeneity in dolomite reservoirs based on CT imaging: a case study of the 3rd member of the Ordovician Yingshan Formation in Well GC601 in Gucheng area, eastern Tarim Basin. Oil & Gas Geology 41 (4): 862-873. https://doi.org/10.11743 /ogg20200418

Zohdi A, Immenhauser A, Rabbani J (2021). Middle Jurassic evolution of a northern Tethyan carbonate ramp (Alborz Mountains, Iran). Sedimentary Geology 416 (15): 1-19. https://doi.org/10.1016/j.sedgeo.2021.105866